

Cite this: DOI: 10.1039/xxxxxxxxxx

Catalysis and tunnelling in the unimolecular decay of Criegee intermediates

Timothy A. H. Burd^a, Xiao Shan^a, and David C. Clary^a

Received Date
Accepted Date

DOI: 10.1039/xxxxxxxxxx

www.rsc.org/journalname

The unimolecular decay of Criegee intermediates is the major producer of OH radicals in the atmosphere. Here, Semi-Classical Transition State Theory (SCTST) in full and reduced dimensions is used to determine thermal rate constants for their unimolecular decay, as well as their decay catalysed by a single water molecule. These reactions shed light on the applicability of SCTST for catalysed hydrogen transfer reactions.

1 Introduction

1.1 Criegee Chemistry

Criegee intermediates (CIs), whose general structure is shown in Fig. 1, are formed by the ozonolysis of alkenes in the atmosphere and are intermediates in a number of critical atmospheric reaction pathways^{1,2}. The branching between these various reaction paths is key in determining the overall effects of CIs on the atmosphere; for example it is thought the majority of atmospheric OH radical production is a result of CI decomposition³. As a result, the reactivity of these species has been the subject of extensive experimental and theoretical studies in recent years^{4–11}.

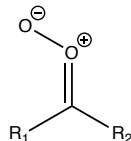
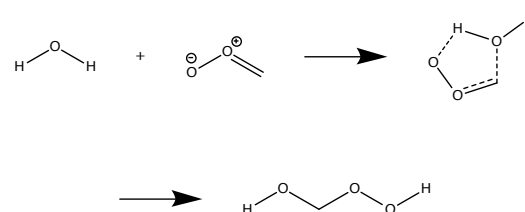
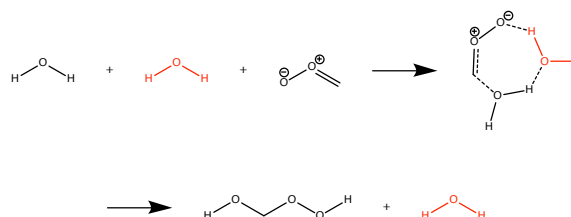


Fig. 1 Representation of a criegee intermediate

After the CIs are formed, they can react bimolecularly with other atmospheric molecules, the “Criegee scavengers”, (H_2O ^{8,12–14}, NO_2 ^{12,15}, SO_2 ^{12,15,16}) or with another CI^{17,18}. One scavenger of particular interest is atmospheric water. Water has been shown to be capable of catalysing several gas-phase reactions^{19–23} and various reactions of CIs have also been found to be catalysed by atmospheric water^{6,24,25}. The reaction of CIs with water as a scavenger (an example of which is shown in Fig. 2) has been shown to have a quadratic rate dependence on the con-



(a) Reaction with a single water molecule



(b) Reaction with two water molecules (Catalytic)

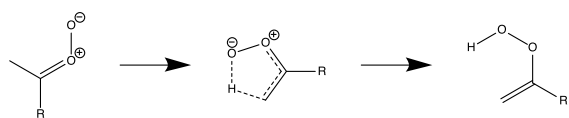
Fig. 2 ‘Scavenger’ reaction of a CI with water.

centration of water, suggesting two water molecules are involved in the reaction^{8,9,13,26}. This has been backed up by theoretical studies^{25,27–30} which have shown the extra molecule completely removes the reaction barrier. This is likely the major atmospheric sink of $\text{H}_2\text{COO}^{13}$.

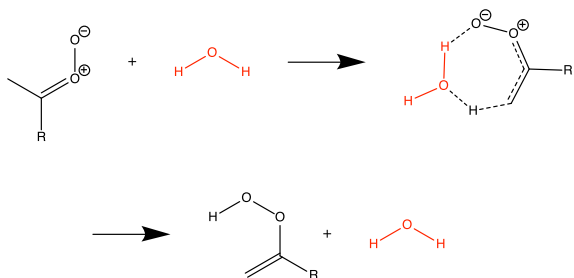
CIs are also susceptible to unimolecular decay, either via three membered ring transition states³¹ or, if there is a syn-alkyl hydrogen, via a 1,4 hydrogen transfer reaction, as shown in Fig. 3 (a), and as studied experimentally and theoretically by Fang *et al.*³². This reaction has the potential to be catalysed by water, as shown in Fig. 3 (b). These catalysed reactions have

^a Physical and Theoretical Chemical Laboratories, South Parks Road, Oxford.; E-mail: timothy.burd@chem.ox.ac.uk

† Electronic Supplementary Information (ESI) available: [details of any supplementary information available should be included here]. See DOI: 10.1039/b000000x/



(a) 1,4 hydrogen transfer reaction



(b) One Water (Catalytic) - Same reaction as in (a), but with a single water molecule in the transition state, shown in red.

Fig. 3 Unimolecular decay pathways of the criegee intermediate.

previously been studied theoretically by Anglada *et al.*²⁷ and Long *et al.*³³ using Variational Transition State Theory with tunnelling corrections.

In this work we study the unimolecular decomposition of the CIs with R=Me ('methylated') and R=H ('unmethylated') as well as the reaction of the unmethylated species catalysed by a single water molecule ('unmethylated, catalysed').

1.2 Semi-classical Transition State Theory

Theoretical studies of atmospheric processes can aid in understanding experimental results, building kinetic models of the atmosphere and predicting reaction pathways. Many atmospheric reactions of interest involve molecules that are too large to be studied with fully quantum methods^{34,35}, as these methods require construction of a large, multi-dimensional potential energy surface (PES), and solving the full-dimensional nuclear Schrödinger equation on this surface³⁶. Efficient methods to study certain aspects of a reaction, for example rate constants, have thus been developed. The simplest of these is Transition State Theory (TST), which neglects recrossing and quantum effects such as tunnelling. Variational Transition State Theory (VTST), as developed by Truhlar and coworkers³⁷, improves upon TST by variationally optimising the transition state dividing surface to find the position of minimum reactive flux, thus minimising recrossings. VTST requires a semi-local potential energy surface around the transition state saddle point. Quantum tunnelling is readily treated in VTST³⁸ using either a 1D-Eckart potential, or in multi-dimensions to account for corner cutting effects³⁸.

Other efficient rate theories have also been developed. Instanton theory³⁹, for example, provides an efficient way to calculate the rate, if the PES in the vicinity of the transition state is known⁴⁰. The rate is calculated by determining the dominant tunnelling path, which is a first-order saddle point of

the Euclidean action. The path is obtained variationally, allowing for 'corner cutting' effects when the dominant tunnelling pathway deviates from the transition state. Fluctuations from the path are treated harmonically. Since the tunnelling pathway is, in general, temperature dependent, the path must be re-optimised at each temperature for which a rate is required.

Semi-classical Transition State Theory (SCTST) uses the semi-classical Bohr-Sommerfeld quantisation to relate the vibrational configuration of the transition state to its barrier penetration integral within the WKB approximation. Like TST, SCTST requires only two molecular geometries to be identified and analysed: the 'reactant' state, and the 'transition' state (TS). Since the tunnelling barrier is not a function of temperature, no additional *ab initio* calculations are required to determine the rate constant for multiple temperatures. This form of SCTST, developed by Miller *et al.*⁴¹⁻⁴³, requires calculation of all third order derivatives, and semi-diagonal fourth order derivatives, of the PES at the transition and reactant states.

This Full-Dimensional SCTST can become prohibitively expensive in computer time for large molecules with many degrees of freedom, as the number of required third and fourth derivatives increases rapidly. Moreover, in order to calculate the rate constants from state-dependent reaction probabilities, all the possible vibrational states of the transition state must be summed over. The number of such states scales exponentially with the system size, and this sum becomes very expensive to compute for even medium sized molecules. The Wang-Landau algorithm⁴⁴ and its implementation for parallel architectures⁴⁵ have been employed to tackle the latter of these two scaling problems, however the anharmonic derivative calculations remains a significant computational expense⁴⁶.

An alternative approach to Full Dimensional SCTST (FD-SCTST) is to use SCTST within a reduced dimensionality (RD) framework⁴⁶⁻⁵⁰. In the simplest model, 1D-SCTST, only the reaction mode is treated as anharmonic, while the remaining 'spectator' vibrational modes are treated using a simple harmonic oscillator model⁴⁸. The computation cost is dramatically reduced, whilst maintaining accurate results in comparison to the full dimensional calculation. Only two derivatives of the PES are required - third and fourth order derivatives along the reaction mode. In addition, the full set of vibrational states can be enumerated with very little computational cost^{44,46}.

The unimolecular decay of CIs, shown in Fig. 3, provide interesting challenges to the rate constant calculations. The reactant molecule contains an internal rotational degree of freedom (the reactive methyl group) that becomes constrained in the TS. Careful treatment of this mode is therefore likely to be critical. In addition, in the large cyclic TS of the H₂O catalysed reaction, several low frequency, and hence large amplitude, vibrational modes exist. A normal harmonic treatment to their vibrational partition functions may be inaccurate. Since these modes only appear in the transition state (i.e. they are not present in the

reactant state), the effect of these modes on the reaction is expected to be significant. Finally, the catalysed reaction involves the transfer of two hydrogen atoms, rather than one, a form of reaction on which SCTST has not previously been tested. In this work, 1D and FD results are compared to experiment in order to evaluate the accuracy of SCTST and the importance of treating anharmonicity in these reactions. In addition, we also assess treating anharmonicity at various levels of electronic structure theory. The findings suggest a procedure for applying SCTST to catalysed unimolecular reactions with reasonable computational expense.

This paper is organised as follows: In section 2, the mathematical background of SCTST in full and one dimension is discussed. Section 3 described the computational details used in the calculations, and section 4 details the results and key findings of this work. Section 5 discusses the key conclusions and outlines plans for further work.

2 Theory

2.1 Semi-classical Transition State Theory (SCTST)

A full description of the SCTST method in full and reduced dimensions was presented by Greene *et al.*⁵¹. Here, we will provide a brief overview and describe our own implementation of the method.

SCTST, as developed originally by Miller *et al.*⁴¹, uses the Bohr-Sommerfeld theory to relate the F^{th} action variable of a quantum system to the path integral of the momentum p_F :

$$h(n_F + 0.5) = \oint p_F dq_F \quad (1)$$

By writing the momentum in terms of the total energy and the effective potential for some vibrational configuration $\{n\}$,

$$p_F = \left[E_v - V_{\{n\}'}(q_F) \right]^{1/2} \quad (2)$$

the path integral can be shown to be proportional to the barrier penetration integral $\theta_{\{n\}'}(E_v)$, where the F^{th} degree of freedom corresponds to the reaction mode in a transition state:

$$h(n_F + 0.5) = \frac{i}{\pi} \theta_{\{n\}'}(E_v) \quad (3)$$

Second order vibrational perturbation theory (VPT2) is then used to write the total energy in terms of the F action variables:

$$E_{\{n\}} = \sum_{i=1}^F \hbar \omega_i (n_i + 0.5) + \sum_{i < j}^F x_{ij} (n_i + 0.5) (n_j + 0.5) + G_0 \quad (4)$$

Substituting $(n_F + 0.5)$ with the penetration integral, via the relation in equation 3, and rearranging for $\theta_{\{n\}'}(E_v)$ gives:

$$\theta_{\{n\}'}(E_v) = \pi \frac{-\Omega_{\{n\}'} + \left[\Omega_{\{n\}'}^2 + 4x_{FF} (\Delta V_f + G_0 - E_{\{n\}'} - E_v) \right]^{1/2}}{2x_{FF}} \quad (5)$$

where

$$\Omega_{\{n\}'} = \frac{\hbar \omega_F}{i} + \sum_{i=1}^{F-1} \frac{x_{iF}}{i} (n_i + 0.5) \quad (6)$$

The VPT2 constants are calculated using the third and fourth order derivatives of the potential along the normal modes, f_{ijk} and f_{iiij} respectively.⁵²:

$$x_{ii} = \frac{\hbar^2}{16\omega_i^2} \left(f_{iiii} - \sum_{j=1}^i \frac{f_{iiij}^2}{\omega_j^2} \frac{8\omega_i^2 - 3\omega_j^2}{4\omega_i^2 - \omega_j^2} \right) \quad (7)$$

$$x_{ik} = \frac{\hbar^2}{4\omega_i \omega_k} \left(f_{iikk} - \sum_{j=1}^F \frac{f_{iiij} f_{jjkk}}{\omega_j^2} \right) \quad (8)$$

$$+ \sum_{j=1}^F \frac{2f_{ijk}^2 (\omega_i^2 + \omega_k^2 - \omega_j^2)}{\left[(\omega_i + \omega_k)^2 - \omega_j^2 \right] \left[(\omega_i - \omega_k)^2 - \omega_j^2 \right]}, i \neq j$$

and:

$$G_0 = \frac{\hbar^2}{64} \sum_{i=1}^F \frac{f_{iiii}}{\omega_i^2} - \frac{7\hbar^2}{576} \sum_{i=1}^F \frac{f_{iii}}{\omega_i^4} + \frac{3\hbar^2}{64} \sum_{i \neq k} \frac{f_{iik}^2}{(4\omega_i^2 - \omega_k^2) \omega_i^2} \quad (9)$$

$$- \frac{\hbar^2}{4} \sum_{i < j < k} \frac{f_{ijk}^2}{\left[(\omega_i + \omega_k)^2 - \omega_j^2 \right] \left[(\omega_i - \omega_k)^2 - \omega_j^2 \right]}$$

Note that special care must be taken to eliminate terms with Fermi resonances⁵³. The state-dependant reaction probability is given by:

$$P_{\{n\}'}(E_v) = \frac{1}{1 + \exp \left[2\theta_{\{n\}'}(E_v) \right]} \quad (10)$$

and the cumulative reaction probability is given by the sum over all state-dependant reaction probabilities at the energy E_v :

$$N(E_v) = \sum_{\{n\}'} P_{\{n\}'}(E_v). \quad (11)$$

Microcanonical rate constants are then given by:

$$k(E) = \frac{N(E)}{2\pi \hbar \rho(E)} \quad (12)$$

where $\rho(E)$ is the density of states in the reactant, whilst thermal rate constants are given by the Boltzman-weighted average of the CRP⁵⁴.

Wagner *et al.*⁵⁵ pointed out this procedure gives qualitatively incorrect results for tunnelling at low energies. The VPT2 procedure reproduces the behaviour of the barrier near the

transition state, but does not incorporate the forward or reverse barrier height, thus giving the incorrect asymptotic tunnelling behaviour. This can be avoided by modelling the potential as a piecewise, continuous, asymmetric Eckart potential that consists of three parts. This potential function maintains the analyticity of $\theta_{\{n\}}(E_v)$ whilst giving the correct asymptotic behaviour. This method also requires calculation of the reverse barrier height, thus the products region must be identified and analysed as well.

In 1D-SCTST, f_{ijk} and f_{iij} are set to zero unless $i = j = k = F$. Thus the reaction mode is not coupled with the rest of the vibrational (spectator) modes in the TS, which are all treated harmonically. This reduces the computational cost of the full dimensional calculation, as numerical derivatives are only required for the reaction mode at the transition state. These derivatives can be estimated cheaply using numerical differentiation. Richardson Extrapolation can be used to improve the results⁵¹, whereby *ab initio* single point energies are calculated at small displacements along the reaction coordinate either side of the transition state.

3 Computational Methods

3.1 *Ab initio* Calculations

Molecular geometries and harmonic frequencies were optimised at the MP2/aug-cc-pVTZ⁵⁶ level of theory in Gaussian 09⁵⁷ using the *tight* convergence criteria.

For the FD calculations, the *freq=anharmonic* keyword was used, at the same level of theory, to determine the \mathbf{x} matrix, as described in detail by Barone⁵². The use of Density Functional Theory (DFT) to determine the anharmonic \mathbf{x} matrix was also tested, using the B3LYP functional⁵⁸ with the aug-cc-pVTZ basis set, and a geometry optimised at this level of theory. DFT second, third and fourth derivatives were used in the calculation of the \mathbf{x} matrix.

For the 1D calculation, x_{FF} was determined from 9 MP2 single point energies along the reaction coordinate, in the vicinity of the transition state, and using second order Richardson extrapolation as described by Greene *et al.*⁵¹. Previous studies^{49,51} have suggested this order of extrapolation is sufficient to give converged derivatives for a typical barrier. A step size of $\Delta Q = 0.05$ (a.m.u.)^{0.5} a_0 was used.

For the water catalysed reaction, which has two, nearly degenerate transition states, only one transition state, was analysed with full dimensional VPT2 at MP2 level, due to the large cost of this calculation. For the 1D rate, the contribution from each TS was nearly identical, so it was assumed the FD contribution from each TS was approximately equal, and the total rate can be calculated as twice the rate through one transition state.

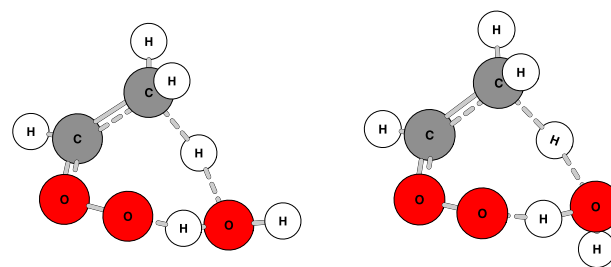


Fig. 4 Two transition state structures of the unmethylated, water catalysed reaction.

3.2 Treatment of hindered rotational degrees of freedom

Internal rotational degrees of freedom present a challenge for rate theories. In the low temperature limit they behave as harmonic oscillators, and in the high temperature limit they behave as free rotors. The partition function can be approximated either as simple harmonic oscillator, or through an approximate expression⁵⁹, which moves smoothly from the harmonic oscillator limit, to the free rotor limit. Both these methods are tested here.

The reactant and transition states include three dihedral angles, which can, in principle, be treated as internal rotors. The first is a rotation about the central C-O bond, with significant double bond character - this has a very high barrier to rotation (120 kJ / mol¹), and so can be safely considered as a harmonic vibration rather than a rotor. The second is the rotation of the reactive methyl group. Since this rotation is constrained in the transition state, its treatment is expected to be critical and a method was employed which has previously been shown⁵⁰ to treat rotating methyl groups accurately in reactive systems. The third is the non-reactive methyl group in the methylated CI species. Both possible hindered rotor treatments will be tested on the two latter internal rotational degrees of freedom.

4 Results and Discussion

4.1 Stationary Point Analysis

Optimised structures for all the relevant Criegee species described in Fig. 3 can be found in the Supplementary Information. Two nearly degenerate transition state structures were found for the water catalysed reactions, corresponding to the external water hydrogens pointing 'up' or 'down' in the seven-membered ring, as shown in Fig. 4; thus the total reaction rate can be found as the sum of the rates through each of these transition states. All the transition states identified are chiral, and so correspond to two degenerate reaction pathways passing through each. Harmonic frequencies at key stationary points are listed in Table 1 and values of x_{FF} and G_0 are compared in full and one dimension in Table 2.

4.2 Hindered Rotor

The unmethylated reaction has a single hindered rotor degree of freedom in the reactant state. 1D-SCTST rates were calculated using harmonic and anharmonic treatments of this mode. Unlike

Table 1 Harmonic frequencies calculated at the MP2/aug-cc-pVTZ level for key stationary point (cm^{-1})

Reactant, R = H					
3253	3207	3102	3048	1515	1474
1457	1398	1296	1131	1031	996
940	745	699	481	304	224
Reactant, R = Me					
3202	3192	3142	3116	3069	3055
1560	1498	1489	1476	1454	1417
1398	1325	1094	1069	991	947
931	830	624	490	352	318
290	209	170			
Transition State, R = H					
1523 i					
3252	3237	3117	1875	1558	1505
1360	1282	1224	1037	1010	970
858	771	746	533	518	
Transition State, R = Me					
1501 i					
3240	3188	3161	3119	3078	1891
1566	1530	1491	1480	1417	1377
1352	1093	1057	1006	990	955
872	758	674	549	515	358
290	136				
Transition State + H ₂ O, R = H					
1587 i					
3831	3271	3195	3142	1745	1650
1632	1573	1448	1368	1325	1264
1203	1037	1022	932	886	766
677	654	598	508	434	415
312	192				

Table 2 Transition State data. All values in cm^{-1} .

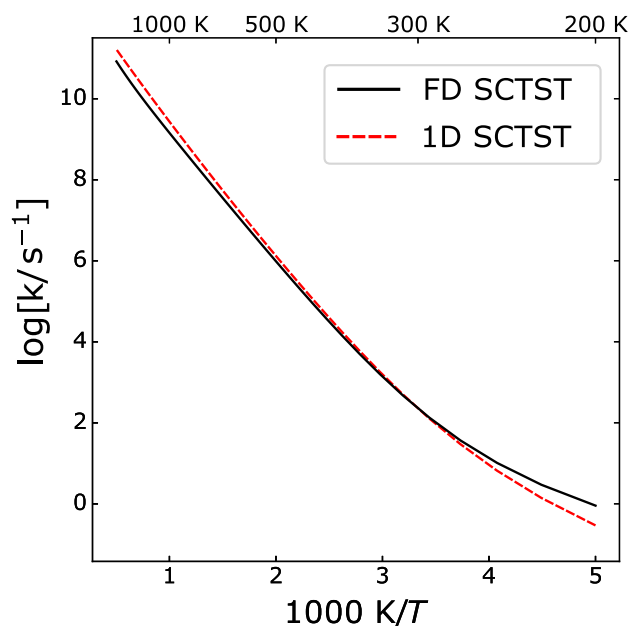
TS	ω_{reaction}	x_{FF} (1D)	G_0 (1D)	x_{FF} (FD)	G_0 (FD)
Uncatalysed					
R=H	1523	-95.67	-19.49	-82.30	-24.86
R=Me	1501	-100.8	-20.80	-90.64	-15.53
Water Catalysed					
R=H	1587	-193.1	-34.01	-115.0	-13.12

in previous studies⁵⁰ the difference between the harmonic model, and a hindered rotor treatment is very small, differing at most by 10% at the highest temperatures studied in this work, and by less than 0.1% at 298 K. This is owing to the relatively high frequency of the rotation mode (224 cm^{-1}) a result of the interaction between the methyl group and the oxygen atoms, hindering rotation at all but the highest temperatures, and the large reduced moment of inertia of the rotation due to the heavy oxygen atoms.

For the methylated reaction, treating the external methyl group also has a negligible effect. Here the effect is small because the differences in partition functions largely cancel out between the reactant and transition state. The rates differ by less than 2% at 298 K.

4.3 Effect of Anharmonicity

The effect of vibrational anharmonicity can be assessed by comparing 1D and FD SCTST rates, as the 1D method neglects anharmonicity in all but the reactive mode. The thermal rate constants are compared in Fig. 5 for the unmethylated reaction,

**Fig. 5** Unimolecular criegee intermediate decay rates in full and one dimension, for the unmethylated reaction

as well as in Fig. 7 for the methylated reaction. It can be seen that for both reactions, 1D-SCTST slightly underestimates tunnelling at temperatures below 300 K, but gives very accurate rate constants in the range 300-2000 K. At 298 K, the 1D and FD results differ by just 38% and 15% for the methylated and unmethylated reactions respectively.

For a large system, the calculation of the anharmonic constant matrix, \mathbf{x} , is the most expensive part of the FD-SCTST calculation, but in general the calculated rate has a weaker dependence on these values than the energy barrier (here calculated at CCSD(T) level of theory) and the harmonic frequencies (here calculated at MP2 level of theory). We investigated using cheaper methods of electronic structure theory to calculate the \mathbf{x} matrix. Fig. 6 shows a comparison of MP2 and DFT methods to calculate the \mathbf{x} matrix. The DFT calculation, despite taking less than one tenth of the computer time, gives excellent agreement with MP2, even at low temperatures where the 1D rate was less accurate. This suggests DFT should be reliable in calculating the \mathbf{x} matrix for SCTST calculations.

4.4 Comparison to Experiment

Chhantyal-Pun *et al.*⁶¹ directly measured the rate of the thermal unimolecular decay of $(\text{CH}_3)_2\text{COO}$ at 293 K using cavity ring-down experiments. The same reaction was studied by Smith *et al.*⁶² between 283 K and 303 K using time resolved UV absorption. Their measured rate constants are compared to SCTST in full and one dimension in Fig. 7. Also presented are the VTST with small curvature tunnelling corrections results of Long *et al.*³³. It is clear that 1D- and FD- SCTST give good agreement both with one another and with the available experimental data, especially for these relatively cheap calculations. Quantum tun-

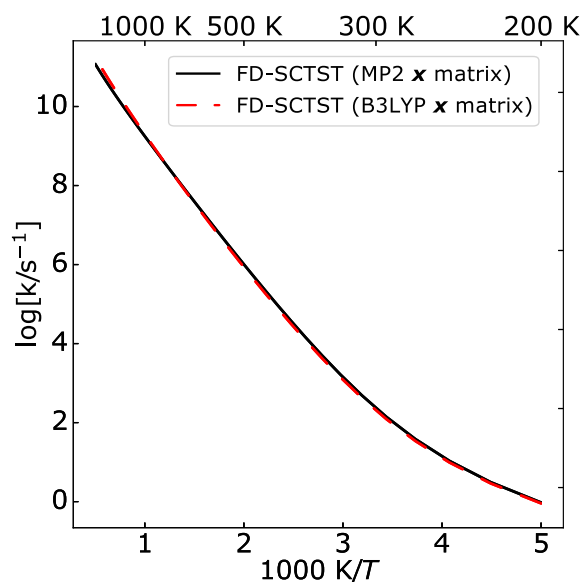


Fig. 6 Two methods of calculating x matrix contributions to the VPT2 energy for the unmethylated, uncatalysed reaction

nelling dominates the rate at low temperatures, as seen by the difference between the TST and SCTST results. Thus the 1D approximation here performs accurately, despite a dramatic cost reduction compared to FD-SCTST. SCTST can also be seen to perform well compared to VTST at low temperatures, where deep tunnelling is significant.

4.5 Effect of Substituent Groups

By comparing the rates of the methylated and unmethylated reactions, the effects of changing the spectator R group on the reaction can be established. Both are compared in Fig. 8. The addition of the Me group slightly increases the rate of reaction. This effect can be attributed to two factors - first, the lowering of the reaction barrier with the methyl group, from 68 kJ/mol to 65 kJ/mol, and second, the harmonic frequency of the methyl group rotor is lower in the transition state than the reactant state, increasing the entropy of the transition state, reducing the entropic barrier. When the transition state forms, the ring formation pulls adjacent groups away from the methyl group, reducing steric interactions, and lowering the species relative energy, as well as the rotor frequency.

4.6 Water Catalysis

The addition of a water molecule to the transition state can be seen to dramatically reduce the energy barrier to reaction from 68 kJ/mol to 33 kJ/mol, as well as reducing the width of the barrier, as shown in Fig. 9. The change barrier width can be attributed to the large change in the anharmonic constant, x_{FF} .

The rates calculated by 1D-SCTST and FD-SCTST calculations are shown in Fig. 10. In contrast to the uncatalysed reaction,

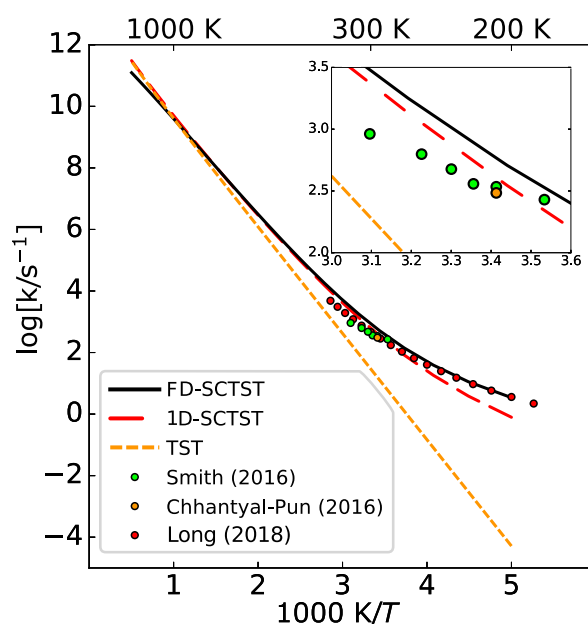


Fig. 7 Results for the methylated, uncatalysed decomposition reaction. Comparison of experimental measurements (Chhantyal-Pun⁶¹ and Smith⁶²) and other theoretical results (Long)³³ with TST and SCTST in full and one dimensions (this work). The inset shows more clearly the comparison of this work to experiment.

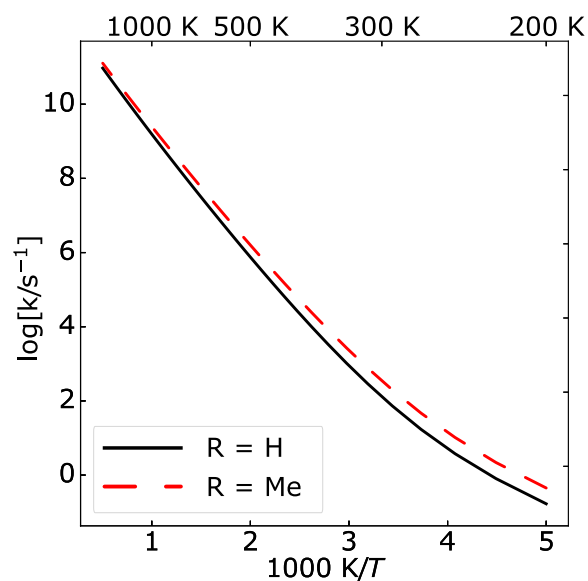


Fig. 8 Effects of methylation on the rate of unimolecular decay on the uncatalysed reaction, calculated using 1D-SCTST

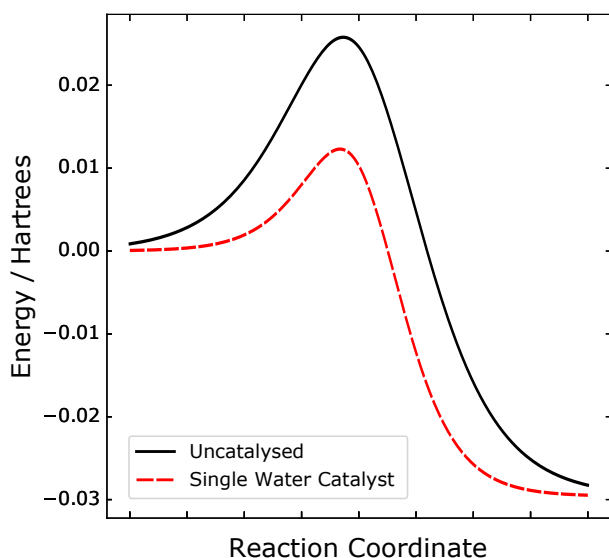


Fig. 9 1D-SCTST effective barrier shapes for the uncatalysed and catalysed unmethylated reactions. Since the two transition states in the catalysed reaction are nearly degenerate, only one barrier is shown.

1D-SCTST fails to accurately predict the rate at low temperatures, particularly lower than 350 K. At 298 K, 1D-SCTST underestimates the rate by about a factor of three. Using DFT to calculate the x matrix dramatically reduces the computational cost (by about a factor of ten in this example), yet gives a very good estimate of the rate over the whole temperature range.

The origin of the discrepancy for the water catalysed reaction between the 1D and FD methods can be attributed to three possible causes:

1. Coupling between the non-reactive modes (x_{ij} with $i, j \neq F$) is non-negligible
2. The coupling between the reactive and non-reactive modes (x_{iF} with $i \neq F$) is non-negligible
3. The 1D estimate of x_{FF} is poor

The first of these manifests itself in the difference in the harmonic and anharmonic vibrational partition functions of the reactant and transition state. The partition functions were found to be very similar over the whole temperature range, such that this cannot be the major source of the difference. These results are detailed in the Supplementary Information. It is interesting that the harmonic treatment performs so well for the transition state, given the presence of several low frequency ring bending modes.

The significance of the remaining two sources of error can be determined by performing a 1D-SCTST calculation using the FD value of x_{FF} , the results of which are shown in Fig. 11. Clearly, using the full-dimensional value of x_{FF} recovers a large amount of the difference. The remainder can be largely attributed to

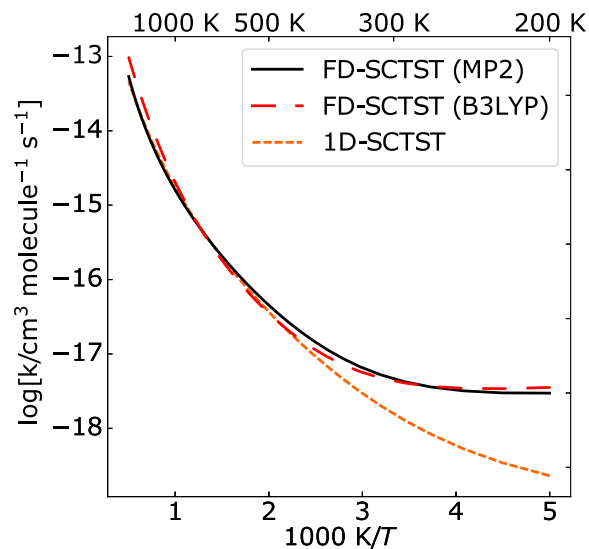


Fig. 10 Comparison of 1D-SCTST, FD-SCTST for the uncatalysed reaction

coupling between the non-reactive modes and the reactive mode. The reason for the discrepancy between FD and 1D values of x_{FF} can be investigated.

The FD value of x_{FF} , is given by:

$$x_{FF} = \frac{\hbar^2}{16\omega_F^2} \left(f_{FFFF} - \sum_{j=1}^F \frac{f_{FFj}^2}{\omega_j^2} \frac{8\omega_F^2 - 3\omega_j^2}{4\omega_F^2 - \omega_j^2} \right) \quad (13)$$

which, under the one-dimensional approximation, becomes:

$$x_{FF} = \frac{\hbar^2}{16\omega_F^2} \left(f_{FFFF} - \frac{5f_{FFF}^2}{3\omega_F^2} \right) \quad (14)$$

For the 1D calculation, derivatives of the form f_{FFi} , with $i \neq F$, are neglected. Fig. 12 shows the values of these derivatives for both the catalysed and uncatalysed transition states, as well as their values as calculated using DFT. From inspecting Fig. 12, it is clear that for the uncatalysed transition state, only one non-reactive mode couples strongly to the reaction mode through the third order derivative. This mode corresponds to the movement of the reactive hydrogen perpendicular to the reaction direction, out of the plane of the ring. In contrast, for the catalysed reaction, many modes couple strongly to the reactive mode, all of which correspond to the in-ring hydrogen atoms moving out of the plane.

Finally, the error due to neglecting x_{iF} is investigated. In Fig. 13, we show the values of x_{iF} calculated at MP2 and B3LYP level of theories for both the catalysed and uncatalysed transition states. Once again, for the uncatalysed species, only one x_{iF} has a significantly large value. It corresponds to the same spectator mode as we found in Fig. 12. On the other hand, several

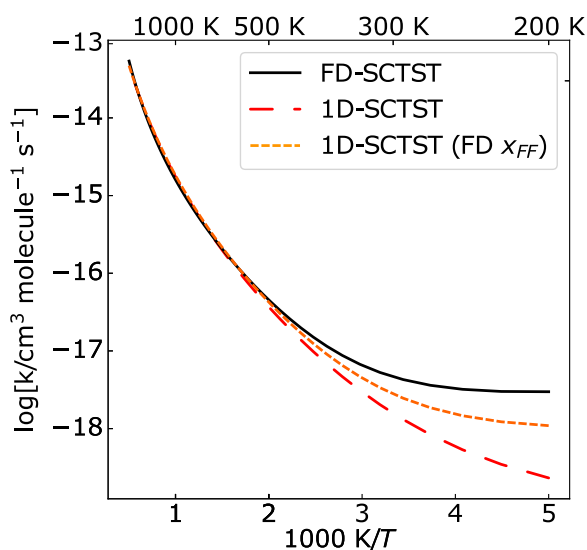


Fig. 11 Comparison of FD-SCTST, 1D-SCTST and 1D-SCTST using the FD value of x_{FF} for the unmethylated, catalysed reaction.

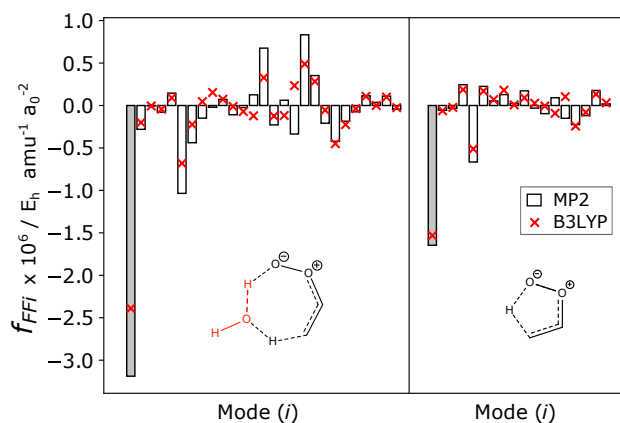


Fig. 12 Comparison of derivatives contributing to the calculation of x_{FF} . Modes are in order of descending frequency, and the pure reaction mode derivative (f_{FF}) is highlighted in grey.

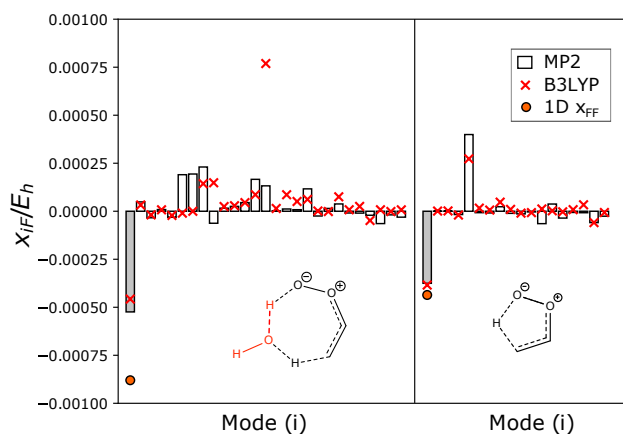


Fig. 13 Comparison of values of x_{iF} for the catalysed and uncatalysed reaction. The reaction mode anharmonic constant (x_{FF}) is highlighted in grey, and the 1D value of x_{FF} is shown as a circle.

spectator modes are found to be strongly coupled to the reaction mode in the catalysed transition state.

4.6.1 Vibrational Locality

One possible way of understanding these differences between the catalysed and uncatalysed reactions is by comparing the ‘locality’ of the reactive modes. The catalysed reaction has two atoms contributing significantly to the reaction mode, whereas the uncatalysed reaction has just one. This allows more of the non-reactive degrees of freedom to interact strongly with the reaction mode, increasing the likelihood of coupling to many modes. This suggests a simple criteria for predicting the success of 1D-SCTST; if the reaction mode is simple, and highly localised, higher order couplings are likely to be smaller, and so 1D approaches are valid. For complex, delocalised reaction modes, this may not be the case.

The locality of a mode, \mathbf{Q} , can be defined as⁶³:

$$\zeta(\mathbf{Q}) = \sum_i (C_i)^2 \quad (15)$$

where C_i corresponds to the contribution of nucleus i to the normal mode \mathbf{Q} :

$$C_i = \sum_{\alpha=x,y,z} (Q_{i\alpha})^2. \quad (16)$$

C_i also corresponds to the fraction of the kinetic energy of atom i in the normal mode. Thus ζ is large for modes in which only one atom contributes significantly, and low for modes in which many atoms are moving together. Its maximal value is one, when only a single atom has a contribution.

Fig. 14 shows the values of C_i for both reaction modes, as well as the overall value of ζ . It is clear that the catalysed reaction has a significantly less localised reactive mode, as a result of two hydrogens being transferred, rather than one.

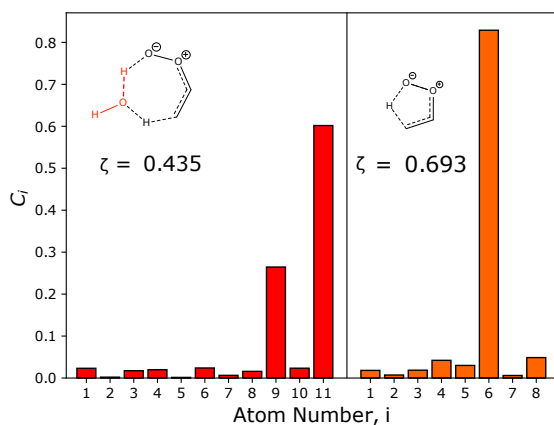


Fig. 14 Locality of the two reactive modes. The atoms with large G_i correspond to the hydrogen atoms being transferred.

The relation between the localisation of a vibrational mode, and its coupling to other modes has been explored in the context of optimising coordinate systems for anharmonic vibrational spectra^{63–65}. It has been shown that using a coordinate system that maximises the locality of the modes speeds up the convergence of the n -mode expansion of the energy *i.e.* localised modes have weaker inter-mode couplings at third and fourth order. This relation between locality and inter-mode coupling may indicate that it is possible to predict how strongly the reactive mode couples to other modes (and thus if the 1D approximation is valid) by calculating the locality of this mode.

4.7 Improving 1D-SCTST

The significant improvement of 1D-SCTST when the FD value of x_{FF} is used, demonstrated in Fig. 11, motivates further developments of the method. It is possible to obtain all the required derivatives to calculate the FD value of x_{FF} with just two additional Hessian matrices displaced along the reaction mode:

$$f_{Fij} = \frac{H_{ij}(\delta Q_F) - H_{ij}(-\delta Q_F)}{2\delta Q_F} \quad (17)$$

and

$$f_{FFii} = \frac{H_{ii}(\delta Q_F) + H_{ii}(-\delta Q_F) - 2H_{ii}(0)}{\delta Q_F^2} \quad (18)$$

where $H_{ij}(\delta Q)$ is element (i, j) of the Hessian matrix calculated at a geometry displaced from the transition state by a distance δQ . As shown in Fig. 13, this can offer a substantial improvement, for only modest additional cost. The values of x_{FF} calculated in this way, for both the catalysed and uncatalysed transition states, are within 0.5% of the values calculated in the normal full-dimensional calculation. For the uncatalysed reaction, this method also brings the 1D results closer to the FD results.

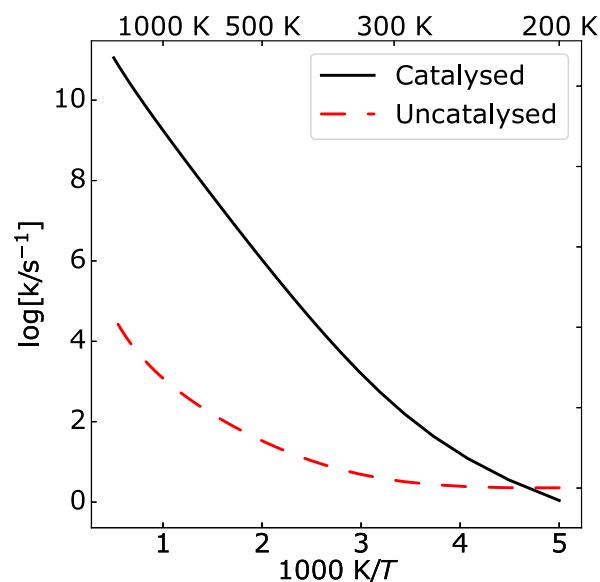


Fig. 15 FD-SCTST rates comparing uncatalysed and catalysed un-methylated reaction at atmospheric water concentration.)

4.8 Catalysis in the Atmosphere

The effective first order rate constant for the decomposition of the Criegee Intermediate in the atmosphere can be written as:

$$k_{pseudo}^{1st} = k_{uncatalysed}^{1st} + k_{catalysed}^{2nd} [\text{water}]_{\text{atmosphere}} \quad (19)$$

where the first term corresponds to the uncatalysed contribution, and the second term corresponds to the catalysed contribution. Their respective contributions are shown in Fig. 15, where an atmospheric water concentration⁶⁰ of $7.0 \times 10^{17} \text{ cm}^{-3}$ was used. This figure suggests that at atmospheric temperatures, the water catalysed reaction has a significant contribution to the total rate, and so cannot be ignored in models of these pathways.

5 Conclusions

The uncatalysed unimolecular decay of two simple Criegee Intermediates have been investigated using Semi-Classical Transition State Theory in full and one dimension. 1D-SCTST, whilst being significantly cheaper, reproduces well the full dimensional rate constant. Both methods also give good agreement with available experimental data, suggesting SCTST is a reliable predictor at a range of temperatures and for related reactions.

We have also shown that 1D-SCTST rate constants do not compare well with the FD rates for for the water catalysed reaction. This is a result of strong coupling of the reaction mode to other ‘spectator’ modes, which can be understood in terms of the delocalisation of the reactive mode. We have shown that the accuracy in the 1D-SCTST can be improved by using an approximate full-dimensional method where only derivatives with at least one index corresponding to the reaction mode are included.

It was shown that water catalysis has a significant impact on the overall rate of Criegee Intermediate decomposition under atmospheric conditions. As well as its inherent interest, understanding how a small number of water molecules can act catalytically in gas phase reactions is also key to understanding solution phase reaction dynamics, where explicit solvent-solute interactions can significantly alter how the reaction proceeds. Understanding these interactions will be key to developing rate theories for the condensed phase.

Conflicts of interest

There are no conflicts to declare

Acknowledgements

X. Shan and D. C. Clary acknowledge financial support from the Leverhulme Trust (Project Grant No. RPG-2013-321). T. A. H. Burd is grateful for support from the EPSRC Centre for Doctoral Training in Theory and Modelling in Chemical Sciences (Project Grant No. EP/L015722/1).

Notes and references

- 1 David Johnson and George Marston. The gas-phase ozonolysis of unsaturated volatile organic compounds in the troposphere. *Chemical Society Reviews*, 37(4):699–716, 2008.
- 2 Jesse H. Kroll, Shailesh R. Sahay, James G. Anderson, Kenneth L. Demerjian, and Neil M. Donahue. Mechanism of HOx Formation in the Gas-Phase Ozone-Alkene Reaction. 2. Prompt versus Thermal Dissociation of Carbonyl Oxides to Form OH. *The Journal of Physical Chemistry A*, 105(18):4446–4457, May 2001.
- 3 R. M. Harrison, J. Yin, R. M. Tilling, X. Cai, P. W. Seakins, J. R. Hopkins, D. L. Lansley, A. C. Lewis, M. C. Hunter, D. E. Heard, L. J. Carpenter, D. J. Creasey, J. D. Lee, M. J. Pilling, N. Carslaw, K. M. Emmerson, A. Redington, R. G. Derwent, D. Ryall, G. Mills, and S. A. Penkett. Measurement and modelling of air pollution and atmospheric chemistry in the U.K. West Midlands conurbation: Overview of the PUMA Consortium project. *Science of The Total Environment*, 360(1):5–25, May 2006.
- 4 Cangtao Yin and Kaito Takahashi. How does substitution affect the unimolecular reaction rates of Criegee intermediates? *Physical Chemistry Chemical Physics*, 19(19):12075–12084, 2017.
- 5 Keith T. Kuwata, Lina Luu, Alexander B. Weberg, Ke Huang, Austin J. Parsons, Liam A. Peebles, Nathan B. Rackstraw, and Min Ji Kim. Quantum Chemical and Statistical Rate Theory Studies of the Vinyl Hydroperoxides Formed in trans-2-Butene and 2,3-Dimethyl-2-butene Ozonolysis. *The Journal of Physical Chemistry A*, 122(9):2485–2502, March 2018.
- 6 Hao-Li Huang, Wen Chao, and Jim Jr-Min Lin. Kinetics of a Criegee intermediate that would survive high humidity and may oxidize atmospheric SO₂. *Proceedings of the National Academy of Sciences*, 112(35):10857–10862, September 2015.
- 7 Manoj Kumar, Daryle Busch, Bala Subramaniam, and Ward Thompson. Barrierless tautomerization of Criegee intermediates via acid catalysis. *Physical Chemistry Chemical Physics*, 16(42):22968–22973, 2014.
- 8 Torsten Berndt, Jens Voigtländer, Frank Stratmann, Heikki Junninen, Roy L. Mauldin Iii, Mikko Sipilä, Markku Kulmala, and Hartmut Herrmann. Competing atmospheric reactions of CH₂OO with SO₂ and water vapour. *Physical Chemistry Chemical Physics*, 16(36):19130–19136, 2014.
- 9 Wen Chao, Jun-Ting Hsieh, Chun-Hung Chang, and Jim Jr-Min Lin. Direct kinetic measurement of the reaction of the simplest Criegee intermediate with water vapor. *Science*, 347(6223):751–754, February 2015.
- 10 Oliver Welz, John D. Savee, David L. Osborn, Subith S. Vasu, Carl J. Percival, Dudley E. Shallcross, and Craig A. Taatjes. Direct kinetic measurements of criegee intermediate (CH₂OO) formed by reaction of CH₂I with O₂. *Science (New York, N.Y.)*, 335(6065):204–207, January 2012.
- 11 L. Vereecken, A. Novelli, and D. Taraborrelli. Unimolecular decay strongly limits the atmospheric impact of Criegee intermediates. *Physical Chemistry Chemical Physics*, 19(47):31599–31612, 2017.
- 12 Yuan-Pern Lee. Perspective: Spectroscopy and kinetics of small gaseous Criegee intermediates. *The Journal of Chemical Physics*, 143(2):020901, July 2015.
- 13 Tom R. Lewis, Mark A. Blitz, Dwayne E. Heard, and Paul W. Seakins. Direct evidence for a substantive reaction between the Criegee intermediate, CH₂OO, and the water vapour dimer. *Physical Chemistry Chemical Physics*, 17(7):4859–4863, 2015.
- 14 Mica C. Smith, Chun-Hung Chang, Wen Chao, Liang-Chun Lin, Kaito Takahashi, Kristie A. Boering, and Jim Jr-Min Lin. Strong Negative Temperature Dependence of the Simplest Criegee Intermediate CH₂OO Reaction with Water Dimer. *The Journal of Physical Chemistry Letters*, 6(14):2708–2713, July 2015.
- 15 Craig A. Taatjes, Oliver Welz, Arkke J. Eskola, John D. Savee, Adam M. Scheer, Dudley E. Shallcross, Brandon Rotavera, Edmond P. F. Lee, John M. Dyke, Daniel K. W. Mok, David L. Osborn, and Carl J. Percival. Direct Measurements of Conformer-Dependent Reactivity of the Criegee Intermediate CH₃choo. *Science*, 340(6129):177–180, April 2013.
- 16 Rabi Chhantyal-Pun, Anthony Davey, Dudley E. Shallcross, Carl J. Percival, and Andrew J. Orr-Ewing. A kinetic study of the CH₂OO Criegee intermediate self-reaction, reaction with SO₂ and unimolecular reaction using cavity ring-down spectroscopy. *Physical chemistry chemical physics: PCCP*, 17(5):3617–3626, February 2015.
- 17 Zachary J. Buras, Rehab M. I. Elsamra, and William H. Green. Direct Determination of the Simplest Criegee Intermediate (CH₂OO) Self Reaction Rate. *The Journal of Physical Chemistry Letters*, 5(13):2224–2228, July 2014.
- 18 Yu-Te Su, Hui-Yu Lin, Raghunath Putikam, Hiroyuki Matsui, M. C. Lin, and Yuan-Pern Lee. Extremely rapid self-reaction of

- the simplest Criegee intermediate CH_2OO and its implications in atmospheric chemistry. *Nature Chemistry*, 6(6):477–483, June 2014.
- 19 Eric T. Aaltonen and Joseph S. Francisco. $\text{HOSO}_2 - \text{H}_2\text{O}$ Radical Complex and Its Possible Effects on the Production of Sulfuric Acid in the Atmosphere. *The Journal of Physical Chemistry A*, 107(8):1216–1221, February 2003.
 - 20 Jaron C. Hansen and Joseph S. Francisco. Radical - Molecule Complexes: Changing Our Perspective on the Molecular Mechanisms of Radical - Molecule Reactions and their Impact on Atmospheric Chemistry. *ChemPhysChem*, 3(10):833–840, October 2002.
 - 21 Robert J. Buszek, Miquel Torrent-Sucarrat, Josep M. Anglada, and Joseph S. Francisco. Effects of a Single Water Molecule on the $\text{OH} + \text{H}_2\text{O}_2$ Reaction. *The Journal of Physical Chemistry A*, 116(24):5821–5829, June 2012.
 - 22 E. Vöhringer-Martinez, B. Hansmann, H. Hernandez, J. S. Francisco, J. Troe, and B. Abel. Water Catalysis of a Radical-Molecule Gas-Phase Reaction. *Science*, 315(5811):497–501, January 2007.
 - 23 Bo Long, Xing-feng Tan, Zheng-wen Long, Yi-bo Wang, Dassen Ren, and Wei-jun Zhang. Theoretical Studies on Reactions of the Stabilized H_2COO with HO_2 and the $\text{HO}_2 - \text{H}_2\text{O}$ Complex. *The Journal of Physical Chemistry A*, 115(24):6559–6567, June 2011.
 - 24 Long Chen, Wenliang Wang, Weina Wang, Yanli Liu, Fengyi Liu, Ning Liu, and Bozhou Wang. Water-catalyzed decomposition of the simplest Criegee intermediate CH_2OO . *Theoretical Chemistry Accounts*, 135(5):131, May 2016.
 - 25 Andrew B. Ryzhkov and Parisa A. Ariya. A theoretical study of the reactions of parent and substituted Criegee intermediates with water and the water dimer. *Physical Chemistry Chemical Physics*, 6(21):5042–5050, October 2004.
 - 26 Liang-Chun Lin, Wen Chao, Chun-Hung Chang, Kaito Takahashi, and Jim Jr-Min Lin. Temperature dependence of the reaction of anti- CH_3CHOO with water vapor. *Physical Chemistry Chemical Physics*, 18(40):28189–28197, October 2016.
 - 27 Josep M. Anglada and Albert Solé. Impact of the water dimer on the atmospheric reactivity of carbonyl oxides. *Physical Chemistry Chemical Physics*, 18(26):17698–17712, June 2016.
 - 28 Long Chen, Wenliang Wang, Liting Zhou, Weina Wang, Fengyi Liu, Chunying Li, and Jian Lü. Role of water clusters in the reaction of the simplest Criegee intermediate CH_2OO with water vapour. *Theoretical Chemistry Accounts*, 135(11):252, November 2016.
 - 29 Liang-Chun Lin, Hung-Tzu Chang, Chien-Hsun Chang, Wen Chao, Mica C. Smith, Chun-Hung Chang, Jim Jr-Min Lin, and Kaito Takahashi. Competition between H_2O and $(\text{H}_2\text{O})_2$ reactions with $\text{CH}_2\text{OO}/\text{CH}_3\text{CHOO}$. *Physical Chemistry Chemical Physics*, 18(6):4557–4568, February 2016.
 - 30 Andrew B. Ryzhkov and Parisa A. Ariya. The importance of water clusters $(\text{H}_2\text{O})_n$ ($n=2, \dots, 4$) in the reaction of Criegee intermediate with water in the atmosphere. *Chemical Physics Letters*, 419(4):479–485, February 2006.
 - 31 Caroline C. Womack, Marie-Aline Martin-Drumel, Gordon G. Brown, Robert W. Field, and Michael C. McCarthy. Observation of the simplest Criegee intermediate CH_2OO in the gas-phase ozonolysis of ethylene. *Science Advances*, 1(2):e1400105, March 2015.
 - 32 Yi Fang, Fang Liu, Stephen J. Klippenstein, and Marsha I. Lester. Direct observation of unimolecular decay of $\text{CH}_3\text{CH}_2\text{OO}$ Criegee intermediates to OH radical products. *The Journal of Chemical Physics*, 145(4):044312, July 2016.
 - 33 Bo Long, Junwei Lucas Bao, and Donald G. Truhlar. Unimolecular reaction of acetone oxide and its reaction with water in the atmosphere. *Proceedings of the National Academy of Sciences*, page 201804453, May 2018.
 - 34 Gunnar Nyman and David C. Clary. Quantum scattering calculations on the $\text{CH}_4 + \text{OH} \rightarrow \text{CH}_3 + \text{H}_2\text{O}$ reaction. *Journal of Chemical Physics*, 101(7):5756–5771, oct 1994.
 - 35 Dong H Zhang and Hua Guo. Recent advances in quantum dynamics of bimolecular reactions. *Annual Review of Physical Chemistry*, 67:135–158, 2016.
 - 36 Dong H. Zhang and Hua Guo. Recent Advances in Quantum Dynamics of Bimolecular Reactions. *Annual Review of Physical Chemistry*, 67(1):135–158, may 2016.
 - 37 Donald G Truhlar and Bruce C Garrett. Variational transition state theory. *Annual Review of Physical Chemistry*, 35(1):159–189, 1984.
 - 38 Jingzhi Pu and Donald G Truhlar. Validation of variational transition state theory with multidimensional tunneling contributions against accurate quantum mechanical dynamics for $\text{H} + \text{CH}_4 \rightarrow \text{H}_2 + \text{CH}_3$ in an extended temperature interval. *Journal of Chemical Physics*, 117(4):1479–1481, 2002.
 - 39 Jeremy O Richardson. Ring-polymer instanton theory. *International Reviews in Physical Chemistry*, 37(2):171–216, 2018.
 - 40 Jeremy O. Richardson. Microcanonical and thermal instanton rate theory for chemical reactions at all temperatures. *Faraday Discussions*, 195(0):49–67, January 2017.
 - 41 William H. Miller. Semiclassical limit of quantum mechanical transition state theory for nonseparable systems. *Journal of Chemical Physics*, 62(5):1899–1906, mar 1975.
 - 42 William H. Miller. Semi-classical theory for non-separable systems: Construction of “good” action-angle variables for reaction rate constants. *Faraday Discussions of the Chemical Society*, 62(0):40–46, jan 1977.
 - 43 William H. Miller, Rigoberto Hernandez, Nicholas C. Handy, Dylan Jayatilaka, and Andrew Willetts. Ab initio calculation of anharmonic constants for a transition state, with application to semiclassical transition state tunneling probabilities. *Chemical Physics Letters*, 172(1):62–68, aug 1990.
 - 44 Thanh Lam Nguyen, John F. Stanton, and John R. Barker. A practical implementation of semi-classical transition state theory for polyatomics. *Chemical Physics Letters*, 499(1-3):9–15, oct 2010.
 - 45 Chiara Aieta, Fabio Gabas, and Michele Ceotto. An efficient computational approach for the calculation of the vibrational density of states. *Journal of Physical Chemistry A*,

- 120(27):4853–4862, 2016.
- 46 Samuel M. Greene, Xiao Shan, and David C. Clary. An investigation of one- versus two-dimensional semiclassical transition state theory for H atom abstraction and exchange reactions. *Journal of Chemical Physics*, 144(8):084113, feb 2016.
- 47 Samuel M. Greene, Xiao Shan, and David C. Clary. Reduced-dimensionality semiclassical transition state theory: Application to hydrogen atom abstraction and exchange reactions of hydrocarbons. *Journal of Physical Chemistry A*, 119(50):12015–12027, dec 2015.
- 48 Samuel M. Greene, Xiao Shan, and David C. Clary. Rate constants of chemical reactions from semiclassical transition state theory in full and one dimension. *Journal of Chemical Physics*, 144(24):244116, jun 2016.
- 49 Xiao Shan, Jack C. Vincent, Sue Kirkpatrick, Maurice D Walker, Mark R. Sambrook, and David C. Clary. A Combined Theoretical and Experimental Study of Sarin (GB) Decomposition at High Temperatures. *Journal of Physical Chemistry A*, jul 2017.
- 50 Timothy A. H. Burd, Xiao Shan, and David C. Clary. Tunnelling and the kinetic isotope effect in $\text{CH}_3 + \text{CH}_4 \rightarrow \text{CH}_4 + \text{CH}_3$: An application of semiclassical transition state theory. *Chemical Physics Letters*, 693:88–94, February 2018.
- 51 Samuel M. Greene, Xiao Shan, and David C. Clary. Rate constants of chemical reactions from semiclassical transition state theory in full and one dimension. *Journal of Chemical Physics*, 144(24):244116, jun 2016.
- 52 Vincenzo Barone. Anharmonic vibrational properties by a fully automated second-order perturbative approach. *Journal of Chemical Physics*, 122(1):014108, jan 2005.
- 53 Vincenzo Barone. Anharmonic vibrational properties by a fully automated second-order perturbative approach. *The Journal of Chemical Physics*, 122(1):014108, December 2004.
- 54 Donald G. Truhlar, Bruce C. Garrett, and Stephen J. Klippenstein. Current Status of Transition-State Theory. *Journal of Physical Chemistry*, 100(31):12771–12800, jan 1996.
- 55 Albert F. Wagner. Improved Multidimensional Semiclassical Tunneling Theory. *Journal of Physical Chemistry A*, 117(49):13089–13100, dec 2013.
- 56 Thom H Dunning Jr. Gaussian basis sets for use in correlated molecular calculations. i. the atoms boron through neon and hydrogen. *Journal of Chemical Physics*, 90(2):1007–1023, 1989.
- 57 M. J. Frisch, G. W. Trucks, H. B. Schlegel, G. E. Scuseria, M. A. Robb, J. R. Cheeseman, G. Scalmani, V. Barone, B. Mennucci, G. A. Petersson, H. Nakatsuji, M. Caricato, X. Li, H. P. Hratchian, A. F. Izmaylov, J. Bloino, G. Zheng, J. L. Sonnenberg, M. Hada, M. Ehara, K. Toyota, R. Fukuda, J. Hasegawa, M. Ishida, T. Nakajima, Y. Honda, O. Kitao, H. Nakai, T. Vreven, J. A. Montgomery, Jr., J. E. Peralta, F. Ogliaro, M. Bearpark, J. J. Heyd, E. Brothers, K. N. Kudin, V. N. Staroverov, R. Kobayashi, J. Normand, K. Raghavachari, A. Rendell, J. C. Burant, S. S. Iyengar, J. Tomasi, M. Cossi, N. Rega, J. M. Millam, M. Klene, J. E. Knox, J. B. Cross, V. Bakken, C. Adamo, J. Jaramillo, R. Gomperts, R. E. Stratmann, O. Yazyev, A. J. Austin, R. Cammi, C. Pomelli, J. W. Ochterski, R. L. Martin, K. Morokuma, V. G. Zakrzewski, G. A. Voth, P. Salvador, J. J. Dannenberg, S. Dapprich, A. D. Daniels, O. Farkas, J. B. Foresman, J. V. Ortiz, J. Cioslowski, and D. J. Fox. Gaussian09 Revision E.01. Gaussian Inc. Wallingford CT 2009.
- 58 P. J. Stephens, F. J. Devlin, C. F. Chabalowski, and M. J. Frisch. Ab Initio Calculation of Vibrational Absorption and Circular Dichroism Spectra Using Density Functional Force Fields. *The Journal of Physical Chemistry*, 98(45):11623–11627, November 1994.
- 59 Yao-Yuan Chuang and Donald G. Truhlar. Statistical thermodynamics of bond torsional modes. *Journal of Chemical Physics*, (112):1221, jan 2000.
- 60 Tianlei Zhang, Rui Wang, Hao Chen, Suotian Min, Zhiyin Wang, Caibin Zhao, Qiong Xu, Lingxia Jin, Wenliang Wang, and Zhuqing Wang. Can a single water molecule really affect the $\text{HO}_2 + \text{NO}_2$ hydrogen abstraction reaction under tropospheric conditions? *Physical Chemistry Chemical Physics*, 17(22):15046–15055, May 2015.
- 61 Rabi Chhantyal-Pun, Oliver Welz, John D. Savee, Arkke J. Eskola, Edmond P. F. Lee, Lucy Blacker, Henry R. Hill, Matilda Ashcroft, M. Anwar H. Khan, Guy C. Lloyd-Jones, Louise Evans, Brandon Rotavera, Haifeng Huang, David L. Osborn, Daniel K. W. Mok, John M. Dyke, Dudley E. Shallcross, Carl J. Percival, Andrew J. Orr-Ewing, and Craig A. Taatjes. Direct Measurements of Unimolecular and Bimolecular Reaction Kinetics of the Criegee Intermediate $(\text{CH}_3)_2\text{COO}$. *The Journal of Physical Chemistry A*, 121(1):4–15, January 2017.
- 62 Mica C. Smith, Wen Chao, Kaito Takahashi, Kristie A. Boering, and Jim Jr-Min Lin. Unimolecular Decomposition Rate of the Criegee Intermediate $(\text{CH}_3)_2\text{COO}$ Measured Directly with UV Absorption Spectroscopy. *The Journal of Physical Chemistry A*, 120(27):4789–4798, July 2016.
- 63 Pawel T. Panek and Christoph R. Jacob. On the benefits of localized modes in anharmonic vibrational calculations for small molecules. *The Journal of Chemical Physics*, 144(16):164111, April 2016.
- 64 Pawel T. Panek and Christoph R. Jacob. Efficient Calculation of Anharmonic Vibrational Spectra of Large Molecules with Localized Modes. *ChemPhysChem*, 15(15):3365–3377, October 2014.
- 65 Andrew Molina, Peter Smereka, and Paul M. Zimmerman. Exploring the relationship between vibrational mode locality and coupling using constrained optimization. *The Journal of Chemical Physics*, 144(12):124111, March 2016.